

This discussion paper is/has been under review for the journal Atmospheric Chemistry and Physics (ACP). Please refer to the corresponding final paper in ACP if available.

# Long-term monitoring of atmospheric total gaseous mercury (TGM) at a remote site in Mt. Changbai area, northeastern China

X. W. Fu<sup>1</sup>, X. Feng<sup>1</sup>, L. H. Shang<sup>1</sup>, S. F. Wang<sup>2</sup>, and H. Zhang<sup>1,3</sup>

<sup>1</sup>State Key Laboratory of Environmental Geochemistry, Institute of Geochemistry, Chinese Academy of Sciences, Guiyang 550002, China

<sup>2</sup>Key Laboratory of Terrestrial Ecological Processes, Institute of Applied Ecology, Chinese Academy of Sciences, Shenyang, China

<sup>3</sup>Graduate University of the Chinese Academy of Sciences, Beijing 100049, China

Received: 17 December 2011 – Accepted: 26 December 2011 – Published: 7 February 2012

Correspondence to: X. Feng (fengxinbin@vip.skleg.cn)

Published by Copernicus Publications on behalf of the European Geosciences Union.

ACPD

12, 4417–4446, 2012

Discussion Paper | Discussion Paper

Long-term monitoring of atmospheric total gaseous mercury

X. W. Fu et al.

Title Page

Abstract

Introduction

Conclusions

References

Tables

Figures

◀

▶

◀

▶

Back

Close

Full Screen / Esc

Printer-friendly Version

Interactive Discussion



## Abstract

Discussion Paper | Discussion Paper | Discussion Paper

ACPD

12, 4417–4446, 2012

## Long-term monitoring of atmospheric total gaseous mercury

X. W. Fu et al.

Total gaseous mercury (TGM) was continuously monitored at a remote site (CBS) in the Mt. Changbai area, northeastern China biennially from 24 October 2008 to 31 October 2010. The overall mean TGM concentration was  $1.60 \pm 0.51 \text{ ng m}^{-3}$ , which is lower than those reported from remote sites in eastern, southwestern and western China, indicating a relatively low regional anthropogenic mercury (Hg) emission intensity in northeastern China. Measurements at a site in the vicinity ( $\sim 1.2 \text{ km}$ ) of the CBS station during August 2005 and July 2006 showed a significantly higher mean TGM concentration of  $3.58 \pm 1.78 \text{ ng m}^{-3}$ . The divergent result was partially attributed to fluctuations in the regional surface wind system and moreover an effect of local emission sources. The temporal variation of TGM at CBS was obviously influenced by regional sources as well as long-range transported Hg. Regional sources, frequently contributing to episodical high TGM concentrations, were pinpointed as a large iron mining district in northern North Korea and two large power plants and urban areas to the southwest of the sampling site. Source areas in Beijing, Tianjin, southern Liaoning, Hebei, northwestern Shanxi and northwestern Shandong were found to contribute to elevated TGM observations at CBS via long-range transport. The diurnal pattern of TGM at CBS was mainly regulated by regional sources, likely as well as intrusion of air masses from the free troposphere during summer season. There are no discernible seasonal pattern of TGM at CBS, which mainly showed links with the patterns of regional air movements and long-range transport.

## 1 Introduction

Mercury (Hg) is a persistent, bio-accumulative and toxic chemical in the environment and has potential adverse effects to human health. Hg in the atmosphere, which is derived from both anthropogenic and natural emission sources, is generally operationally defined into three major forms, namely elemental gaseous mercury (GEM), reactive

[Title Page](#)

[Abstract](#)

[Introduction](#)

[Conclusions](#)

[References](#)

[Tables](#)

[Figures](#)

◀

▶

[Back](#)

[Close](#)

[Full Screen / Esc](#)

[Printer-friendly Version](#)

[Interactive Discussion](#)



5 gaseous mercury (RGM) and particulate mercury (PHg), with the sum of GEM and RGM known as total gaseous mercury (TGM). Due to its high surface reactivity and water solubility, RGM and PHg are readily deposited on a local and/or regional scale. On the contrary, GEM, the most abundant form of Hg in the atmosphere (> 90 %), has an atmospheric residence time of ~0.5–2 yr that is compatible with intra-hemispherical mixing (Schroeder and Munthe, 1998; Lindberg et al., 2007).

10 Recently, significant efforts have been invested into measure atmospheric TGM in remote areas on a global scale and to evaluate the effect of long-range transport, local and regional sources, as well as atmospheric physical and chemical processes on the observations. The mean level of TGM in remote areas of North America and Europe have been reported in the range of 1.3–1.7 ng m<sup>-3</sup> (e.g., Lee et al., 1998; Kellerhals et al., 2003; Poissant et al., 2005; Kock et al., 2005; Choi et al., 2008; Mao et al., 2008; Engle et al., 2010), and for the Southern Hemisphere in the range of 0.9–1.3 ng m<sup>-3</sup> (Temme et al., 2003; Slemr et al., 2008; Brunke et al., 2010). Nevertheless, observations of TGM in many relatively remote areas of East Asia tend to be comparatively elevated (Nguyen et al., 2007; Fu et al., 2008, 2010a, 2011; Wan et al., 2009; Ci et al., 2011). The spatial distribution of atmospheric surface layer TGM can at large be convoluted by using global anthropogenic Hg emission inventories as a reference (Wilson et al., 2006; Pacyna et al., 2011), indicating the anthropogenic Hg sources play a 15 dominant role in the atmospheric TGM distributions.

20 East Asia is ranked as the world's largest anthropogenic source region of atmospheric Hg, where in China the majority (~83 %) of the emissions originates from coal combustion and non-ferrous smelting activities (Wu et al., 2006; Pirrone et al., 2010; Pacyna et al., 2011). The density of anthropogenic Hg emission in China displays a 25 distinct regional distribution pattern with relatively higher emissions in central, eastern, southern and southwestern China. Long-term monitoring of TGM at remote sites is crucial to assess the regional atmospheric Hg budget. A study conducted in a remote region of southwestern China showed a mean TGM concentration of  $2.80 \pm 1.51$  ng m<sup>-3</sup> (Fu et al., 2010), which is clearly elevated compared to the northern hemispherical

## Long-term monitoring of atmospheric total gaseous mercury

X. W. Fu et al.

[Title Page](#)

[Abstract](#)

[Introduction](#)

[Conclusions](#)

[References](#)

[Tables](#)

[Figures](#)

◀

▶

[Back](#)

[Close](#)

[Full Screen / Esc](#)

[Printer-friendly Version](#)

[Interactive Discussion](#)



background ( $1.5\text{--}1.7 \text{ ng m}^{-3}$ , Lindberg et al., 2007; Valente et al., 2007), indicating relatively high anthropogenic Hg emission in the specific region. Nevertheless, long-term studies of atmospheric TGM are very limited in China. Due to the impact of local emissions and strong regional sources, some of the previous studies tend to overestimate the regional background levels of atmospheric TGM (i.e., Fu et al., 2009; Wan et al., 2009). In the present study, we conducted a two year continuous measurement of atmospheric TGM at a remote site in Mt. Changbai area, northeastern China. Based on this long-term dataset, we discuss in this paper the impacts of local and regional sources on the observations. We have used a hybrid receptor model to identify the potential source regions and pathways that contributing to the elevated TGM concentrations in the study area via long-range transport.

## 2 Experimental

### 2.1 Sampling locations

The sampling site (CBS:  $42^{\circ}24'0.9''$  N,  $128^{\circ}06'45''$  E, 741 m a.s.l.) is operated by the Chinese Terrestrial Ecosystem Flux Research Network and situated about 40 km to the north of the major peak of Changbai mountain range (Fig. 1). This mountain range stretches more than 1000 km from southwest to northeast. During the calendar year of 2005–2006, Wan et al. (2009) carried out a one-year measurement of atmospheric TGM in the Open Research Station of Changbai Mountain Forest Ecosystem, Chinese Academy of Sciences (S2, Fig. 1c,  $42^{\circ}24'0.1''$  N,  $128^{\circ}06'25''$  E, 738.1 m a.s.l.), which is in-turn located about 1.2 km to the west of the CBS station.

Regions to the west and south of the sampling site consist of naturally preserved forest and mountainous areas without any significant sources of atmospheric pollutants. Most of the regional large point sources and major settlements are located to the west of the sampling site (Fig. 1c). For example, Baishan city, with a pollution of  $\sim 300\,000$  and a large coal-fired power plant, is located 150 km southwest to the sampling site,

**Long-term monitoring of atmospheric total gaseous mercury**

X. W. Fu et al.

and Tonghua city, with a population of 450 000 and a large coal-fired power plant, is located about 190 km southwest to the sampling site (Fig. 1c). Figure 1a shows the locations of large coal-fired power plants (incl. installed capacity >1000 MW) in East Asia. Most of these large point sources are situated more than 300 km to the west and southwest of our study area. Baihe town, a major settlement in the local area with a population of 49 000, is located about 4 km to the northeast of the sampling site and may constitute a local emission source of Hg.  
5

## 2.2 TGM measurement method

During 24 October 2008 and 31 October 2010, TGM concentration in ambient air was continuously monitored using an automated Hg vapour analyser (Tekran 2537A). The operation of the instrument relying on pre-concentration of TGM onto gold traps, followed by thermal desorption and detection of  $\text{Hg}^0$  by cold vapour atomic fluorescence spectrometry. The instrument features two gold cartridges working in parallel. While one cartridge is collecting TGM, the other one is performing an analysis of the collected 10 TGM. The function of the cartridges is then reversed, allowing continuous sampling of ambient air. The sampling inlet was mounted at a height of 2–3 m above the forest canopy by using a 25 m Teflon tube and a 15 m heated Teflon tube. Particulate matter in ambient air was removed using a 45-mm diameter Teflon filter (pore size 0.2  $\mu\text{m}$ ) upstream of the analyser, which was replaced every two week. The analyser was programmed to measure atmospheric TGM at a time resolution of 5 min and at a sampling 15 flow rate of  $1.0 \text{l min}^{-1}$ . The detection limit of the analyser was determined to about 0.15  $\text{ng m}^{-3}$ . Calibrations of the analyser were invoked automatically every 25 h by means of using the instrument's internal Hg permeation source. The emission rate of the permeation source was verified every 4–6 months by performing manual injections 20 of  $\text{Hg}^0$  by a syringe from an external Hg vapour source (Tekran 2505). During sampling, a standard addition unit (Tekran 1120) was employed to make real-time check of the measurements, and results from the standard addition unit were comparable to the auto calibrations results (ratio =  $1.08 \pm 0.10$ ).  
25

[Title Page](#)[Abstract](#)[Introduction](#)[Conclusions](#)[References](#)[Tables](#)[Figures](#)[◀](#)[▶](#)[◀](#)[▶](#)[Back](#)[Close](#)[Full Screen / Esc](#)[Printer-friendly Version](#)[Interactive Discussion](#)

Hourly averaged meteorological parameters including wind speed and wind direction were retrieved from the station S2 as such measurements were not available at CBS. Since S2 was located about 1.2 km from CBS and the surrounding areas were characterised by flat terrain, the meteorological parameters measured at S2 were used for further analysis at CBS.  
5

### 2.3 Potential Source Contribution Function (PSCF) analysis

To identify the possible impacts of long-range transport on atmospheric TGM, 5-day backward trajectories arriving at CBS at a height of 500, 1000 and 1500 m above ground level were calculated using a Geographical Information System based software  
10 (Wang et al., 2009) and gridded meteorological data from the US National Oceanic and Atmospheric Administration (NOAA).

The calculated backward trajectories were used to make Potential Source Contribution Function (PSCF) analysis of atmospheric TGM at Mt. Changbai, which has been applied in many previous studies to identify possible source areas for the measured  
15 atmospheric pollutants (e.g., Kim et al., 2005; Choi et al., 2008). The PSCF values for the grid cells in the study domain were calculated by counting the trajectory segment endpoints that terminate within each cell. The number of endpoints that fall in the  $i,j$ -th cell is designated as  $N_{ij}$ . The number of endpoints for the same cell corresponding to  
20 TGM concentrations higher than an arbitrarily set criterion (mean TGM concentration during the whole sampling campaign was used here) is defined to be  $M_{ij}$ . The PSCF value for the  $i,j$ -th cell is then defined as:

$$\text{PSCF}_{ij} = M_{ij} \div N_{ij} \quad (1)$$

Since backward trajectories starting at different heights traverse different distances and pathways, multiple height PSCF analysis was performed with starting elevations  
25 of 500, 1000 and 1500 m above ground level, respectively. The total endpoints in the geophysical region covered were 234 998 and the geophysical region was divided into 9801 grid cells of  $0.5 \times 0.5$  latitude and longitude. To reduce the effect of small

<a href="#">Title Page</a>	
<a href="#">Abstract</a>	<a href="#">Introduction</a>
<a href="#">Conclusions</a>	<a href="#">References</a>
<a href="#">Tables</a>	<a href="#">Figures</a>
<a href="#">◀</a>	<a href="#">▶</a>
<a href="#">◀</a>	<a href="#">▶</a>
<a href="#">Back</a>	<a href="#">Close</a>
<a href="#">Full Screen / Esc</a>	
<a href="#">Printer-friendly Version</a>	
<a href="#">Interactive Discussion</a>	

<a href="#">Title Page</a>	
<a href="#">Abstract</a>	<a href="#">Introduction</a>
<a href="#">Conclusions</a>	<a href="#">References</a>
<a href="#">Tables</a>	<a href="#">Figures</a>
<a href="#">◀</a>	<a href="#">▶</a>
<a href="#">◀</a>	<a href="#">▶</a>
<a href="#">Back</a>	<a href="#">Close</a>
<a href="#">Full Screen / Esc</a>	
<a href="#">Printer-friendly Version</a>	
<a href="#">Interactive Discussion</a>	

values of  $N_{ij}$ , the PSCF values were multiplied by an arbitrary weight function  $W_{ij}$  to better reflect the uncertainty in the values for these cells (Polissar et al., 2001). The weighting function reduced the PSCF values when the total number of the endpoints in a particular cell ( $N_{ij}$ ) was less than about three times the average value of the end points per each cell:

$$W_{ij} = \begin{cases} 1.0 & N_{ij} > 3N_{\text{ave}} \\ 0.70 & 3N_{\text{ave}} > N_{ij} > 1.5N_{\text{ave}} \\ 0.40 & 1.5N_{\text{ave}} > N_{ij} > N_{\text{ave}} \\ 0.20 & N_{\text{ave}} > N_{ij} \end{cases} \quad (2)$$

### 3 Results and discussion

#### 3.1 Overall characteristics of TGM distribution in ambient air

Figure 2 shows the time series of atmospheric TGM concentrations from 24 October 2008 to 31 October 2010 at CBS. The majority of the data (75.5 %) fell in the range of 1.0–2.0 ng m<sup>-3</sup>, which is commonly regarded as the values observed at remote sites in the Northern Hemisphere. However, episodes with elevated TGM concentrations were intermittently observed during the whole sampling campaign, by that 18.1 % and 0.2 % of the data exceeded the level of 2.0 and 4.0 ng m<sup>-3</sup>, respectively.

Overall mean TGM concentration at CBS was  $1.60 \pm 0.51$  ng m<sup>-3</sup>. This is significantly lower than the results of previous observational studies conducted at remote sites in Chinese mainland, such as: Mt. Waliguan in northwestern China ( $1.98 \pm 0.98$  ng m<sup>-3</sup>, Fu et al., 2011), Mt. Leigong in southwestern China ( $2.80 \pm 1.51$  ng m<sup>-3</sup>, Fu et al., 2010), Shangri-La observatory in southwestern China ( $2.59 \pm 1.33$  ng m<sup>-3</sup>, Zhang et al., 2011) and Chengshantou marine station in eastern China ( $2.31 \pm 0.74$  ng m<sup>-3</sup>, Ci et al., 2011), but is comparable to those observed from remote areas in Europe and North America ( $1.0 \sim 2.0$  ng m<sup>-3</sup>, e.g., Kock et al., 2005; Poissant et al., 2005; Choi et al., 2008; Mao et al., 2008; Engle et al., 2010). Our

result also compares favourably with the TGM level predicted from modelling studies (Lin et al., 2010; Li et al., 2010). The relatively low TGM level observed at CBS can be explained by a combination of factors. First of all, the study area is relatively isolated from dominant source regions of China. As can be seen from Fig. 1a, most of the large coal-fired power plants (>1000 MW) are located at more than 200 km from the sampling site. Moreover, large industrial centres and urban areas associated with significant anthropogenic Hg emissions are located more than 100 km from the study area (Baihe town was found to have a limited effect on TGM levels at CBS site, which will be further discussed in Sect. 3.2). Moreover, northeastern Asia is regarded as a region with relatively low anthropogenic Hg emissions, which receives background air masses from Siberia and Northern Pacific Ocean (Wilson et al., 2006; Pacyna et al., 2010).

### 3.2 A comparison to a previous monitoring at S2: implication of long-range transport, regional and local impacts

During 5 August 2005 and 5 July 2006, Wan et al. (2009) carried out TGM measurements at the site S2 (~1.2 km to the west of CBS, cf. Fig. 1a and b). The overall mean TGM concentration at S2 was  $3.58 \pm 1.78 \text{ ng m}^{-3}$ , which is more than twofold higher compared to the present study. Given the proximity between the stations, we may hypothesize that the significant inter-stational difference in TGM concentrations is mostly due to an abrupt temporal shift in the source strength of the regional and local sources.

Figure 3a and 3b display the wind rose and TGM concentration distribution as a function of wind direction at CBS, respectively. During the study period 2008–2010, most of the surface air flows were derived from a easterly sector; whereas air flows from southwest to northeast passing over the major regional sources, were encountered at considerably lower frequencies. TGM concentrations exhibited a strong dependence on wind directions at CBS. As shown in Fig. 3b, wind flows from the southwestern sector were frequently associated with elevated TGM concentrations ( $1.6\text{--}1.8 \text{ ng m}^{-3}$ ) than other sectors. This corresponds very well with the locations of the two largest

<a href="#">Title Page</a>	
<a href="#">Abstract</a>	<a href="#">Introduction</a>
<a href="#">Conclusions</a>	<a href="#">References</a>
<a href="#">Tables</a>	<a href="#">Figures</a>
<a href="#">◀</a>	<a href="#">▶</a>
<a href="#">◀</a>	<a href="#">▶</a>
<a href="#">Back</a>	<a href="#">Close</a>
<a href="#">Full Screen / Esc</a>	
<a href="#">Printer-friendly Version</a>	
<a href="#">Interactive Discussion</a>	

**Long-term monitoring of atmospheric total gaseous mercury**

X. W. Fu et al.

[Title Page](#)[Abstract](#)[Introduction](#)[Conclusions](#)[References](#)[Tables](#)[Figures](#)[◀](#)[▶](#)[◀](#)[▶](#)[Back](#)[Close](#)[Full Screen / Esc](#)[Printer-friendly Version](#)[Interactive Discussion](#)

coal-fired power plants and large cities to the southwest of the sampling site (Fig. 1c), which should be the most significant sources of atmospheric TGM in the Mt. Changbai area. However, it should be pointed out that the regional sources to the west were not likely to contribute significantly to the sampling site, mainly because air flows from southwest to northwest constituted a small portion during the study period. On the other hand, air flows from north to west and south showed relatively low TGM concentrations of  $1.4\text{--}1.6\text{ ng m}^{-3}$  (Fig. 3b), with the exception of easterly flow. The slightly elevated TGM mean concentrations associated with easterly flow can potentially be attributed to Hg emissions from Maoshan iron mining area in northern North Korea, which is one of the largest opencast operating iron mining areas in the Northeast Asia located  $\sim 100\text{ km}$  to the east of CBS (Fig. 1). Since air flows from the eastern direction were most abundant, it could be speculated that Hg emissions from the mining area have a relatively high impact on the TGM observations at CBS. On the contrary, we were not able to identify elevated TGM concentrations associated with air flows originated from and/or passed over Baihe town.

Effects of long-range transport of air pollutants on the TGM level at CBS were evaluated by using the PSCF analysis. As shown in Fig. 4, Beijing, Tianjin, northwestern Shanxi, northwestern Shandong, Hebei and southern Liaoning provinces in northern China as well as southern North Korea were identified as potential source regions and pathways that contributed to the CBS sampling site. The distribution of areas with high PSCF values corresponds very well with the anthropogenic Hg emission in eastern Asia (Fig. 4), indicating that long-range transport of Hg from strong source regions influences TGM distribution in ambient air at CBS. Northern central China including Beijing, Tianjin, Shanxi, Hebei, Shandong and Liaoning is an important anthropogenic source region of China, and it was predicted that 140 tons of Hg was emitted in the atmosphere in 2003 (Wu et al., 2006). There is a lack of long-term monitoring studies of ambient TGM in this region, however, a monitoring survey of TGM at rural, suburban and urban sites of Beijing municipality revealed elevated levels (mean range from 3.1 to  $24.7\text{ ng m}^{-3}$ ) of TGM, indicating significant regional sources of this air pollutant (Liu

et al., 2002). The potential area identified in southern North Korea includes several large coal-fired power plants (Fig. 1) and being classified as a high anthropogenic Hg emission region according to emission inventory estimates (e.g., Shetty et al., 2008; Wilson et al., 2006; Pacyna et al., 2010). Northern Bohai Sea was also identified as a potential source region to the CBS. We conclude that this mainly results from anthropogenic Hg emissions from surrounding areas of the Bohai Sea. As shown in Fig. 1a, there are a number of large coal-fired power plants in the coastal areas of Bohai Sea. Besides, there are also a number of large cities and industrial factories (e.g., large Zinc plants, chlor-alkali plants) in this area (Wang et al., 2009; Li et al., 2010).

In contrast, TGM concentrations at S2 during August 2005 and July 2006 were mainly affected by regional and local sources. As shown in Fig. 3c, surface wind system at S2 during October 2005 and July 2006 showed a quite different distribution pattern with CBS, with southwest as the predominant wind direction. Since most of the regional sources were located to the southwest of the sampling site, the predominant southwesterly flow plausibly contributed to the elevated levels of TGM at S2.

Besides, we suggest emissions from coal and biomass burning in the station and the Baihe town also played an important role in TGM distribution at S2. The Changbai mountain forest ecosystem research station is generally open to the scientific researchers during summer season (July to September). During the opening season, coal and biomass burning for cooking is prevalent and releases Hg to the atmosphere. As shown in Fig. 5, TGM concentrations at S2 during the opening season varied significantly and exhibited a much higher mean TGM concentration (mean  $4.49 \pm 2.44 \text{ ng m}^{-3}$ ) compared to other seasons (mean  $3.02 \pm 1.44 \text{ ng m}^{-3}$ ), indicating the significant impact of Hg emissions deriving from inside the research station area.

Nevertheless, in the study of Wan et al. (2009), the highest mean TGM concentrations at S2 were observed under northerly to westerly flow patterns (Fig. 3d), which is not consistent with the results obtained at CBS. This indicates that, unlike the site of CBS in this study, Hg emissions from Baihe town more than likely had a notable impact at S2. Partially, the relative proximity of S2 to Baihe town compared to CBS could result

## Long-term monitoring of atmospheric total gaseous mercury

X. W. Fu et al.

[Title Page](#)

[Abstract](#)

[Introduction](#)

[Conclusions](#)

[References](#)

[Tables](#)

[Figures](#)

◀

▶

[Back](#)

[Close](#)

[Full Screen / Esc](#)

[Printer-friendly Version](#)

[Interactive Discussion](#)



in a larger impact, but it is also plausible that the local coal and biomass burning for domestic heating in recent years has been decreased to yield lower emissions. In general, coal and biomass combustion during cold season are very common in most areas of China. This source has strong seasonal variations with enhanced emissions in cold

5 months and could play an important role in local atmospheric Hg budget. Previous study by Fu et al. (2009) in southwestern China revealed that such sources have an important role in the local atmospheric Hg budget during the cold season by means that the average TGM concentration downwind of a township was  $\sim 2 \text{ ng m}^{-3}$  (25 %) higher compared to that of the upwind air. As shown by Wan et al. (2009), elevated TGM 10 concentrations were observed during cold months at S2, which was partially attributed to the impact of local sources. The impact of emissions from Baihe town on the observations made at S2 site was probably enhanced under the presence of a stable local boundary layer, which corresponded well with the relatively higher TGM concentrations 15 observed at low wind speed (Wan et al., 2009).

15 The PSCF results regarding the observational study at S2 suggest a significant impact from local and regional sources. As shown in Fig. 6, a small region to the north and south of the sampling site were modelled with the highest PSCF value and probably contributed significant to S2. However, this region had a relatively sparse population and there is no significant point source. The high PSCF value generated in this area 20 might be probably due to the trailing effect. In general, PSCF analysis could generate a constant weight along the path of trajectories, and areas downwind and upwind as actual source regions are also likely to be identified as potential source regions. As discussed above, Baihe town, located closely to the north of S2, contributed significantly to the high levels of TGM at S2. This local source could probably be responsible 25 for the high PSCF value in the region to the north of the sampling site. Impact of regional emissions from Baishan and Tonghua on the S2 was not clearly identified by the PSCF result. It is speculated that Hg released from Baishan and Tonghua urban areas was mainly carried to the sampling site via local surface wind system, which may not coincide very well with directions of backward trajectories. Overall, locations

## Long-term monitoring of atmospheric total gaseous mercury

X. W. Fu et al.

[Title Page](#)

[Abstract](#)

[Introduction](#)

[Conclusions](#)

[References](#)

[Tables](#)

[Figures](#)

◀

▶

[Back](#)

[Close](#)

[Full Screen / Esc](#)

[Printer-friendly Version](#)

[Interactive Discussion](#)



of source regions at S2 identified by the PSCF analysis do not correspond very well with large source regions in northeastern and northern China. We suggested that local and regional sources might play a predominant role in TGM distribution at S2 during the sampling campaign, whereas effects from long-range transport might be less important. Moreover, it also indicates that observations made at sites impacted with strong local and regional sources are less suitable to identifying potential source and pathways of pollutants using PSCF method.

### 3.3 Temporal trends of TGM at CBS

TGM concentrations showed clear diurnal variations at CBS. As shown in Fig. 7, TGM concentrations during all the seasons tend to increase after sunrise (05:00–06:00 in local time), with the highest concentrations observed before noon and then decreased throughout the afternoon and the whole night. This is consistent with the observations conducted at remote sites in Mt. Leigong and Mt. Gongga, and also compare favourably to observations at S2 during August 2005 and July 2006. The surface wind system at CBS was partially controlled by mountain and valley breeze, with air flows from surrounding low-altitude areas during daytime and from mountain peaks during night, respectively. We conclude that the elevated TGM concentrations during daytime were plausibly attributable to the impact of regional sources. During night, TGM concentrations in ambient air of the industrial and areas probably increased due to the significant Hg emissions under shallow nocturnal boundary layer conditions (Lee et al., 1998; Feng et al., 2004). The Hg-enriched air masses from regional source regions could be transported to the sampling site via upslope air movements and caused elevated TGM concentrations. The peaks observed before noon were probably due to the encounters of plumes from coal-fired power plants and urban areas, while decrease of TGM after noon was likely caused by enhanced vertical atmosphere movement which diluted the regional atmospheric TGM concentrations.

The diurnal pattern of TGM was especially pronounced during summer, with significantly lower nighttime TGM concentrations compared to other seasons. We speculate

Discussion Paper	Title Page
Discussion Paper	Abstract
Discussion Paper	Introduction
Discussion Paper	Conclusions
Discussion Paper	References
Discussion Paper	Tables
Discussion Paper	Figures
Back	Close
Full Screen / Esc	
Printer-friendly Version	
Interactive Discussion	

that this is mainly linked to downslope flows originated from free troposphere, which may have much lower GEM concentrations due to the fast oxidation of GEM by ozone, OH or possible other oxidants (Swartzendruber et al., 2006; Faïn et al., 2009; Slemr et al., 2009). Also, deposition of TGM on vegetation foliage during leaf-growing season might play an additional effect to decrease night TGM concentrations (Poissant et al., 2008).

TGM concentrations did not show clear seasonal patterns at CBS. As shown in Fig. 8, the highest monthly value was observed in June 2010, with the mean of  $2.14 \text{ ng m}^{-3}$ . However, the monthly mean TGM concentration ( $1.27 \text{ ng m}^{-3}$ ) in June 10 2009 was relatively lower compared to other months. Additionally, during the first year, months during cold seasons generally showed relatively higher TGM concentrations; while TGM concentrations were relatively lower in the cold seasons of the second year (Fig. 8). The seasonal pattern at CBS was quite different from the studies in southwestern China (Feng et al., 2004; Fu et al., 2008, 2010), which showed highly elevated 15 TGM concentrations in cold seasons related to enhanced local and regional coal combustions. We examined the rising wind during June and October 2010 in which the highest monthly mean TGM concentrations were observed ( $2.14$  and  $1.92 \text{ ng m}^{-3}$ , respectively). It is shown that surface wind flows in these two months were mostly from directions linked to the regional sources as aforementioned (Fig. 9). This indicates 20 variations of predominant wind directions, which might change sources-receptor relationships in the study area, playing an important role in influencing monthly TGM variations.

Long-range transport was also responsible for the seasonal variations of TGM at CBS. Figure 10 shows the seasonal PSCF results at CBS. It is shown that the CBS 25 was mostly impacted by anthropogenic Hg emissions of Beijing, Tianjin, Hebei and Liaoning during spring and autumn sampling campaigns during which TGM concentrations were elevated (Table 1). In winter, north of Shanxi province was calculated with the highest PSCF value (Fig. 10d) and this is probably linked to Hg emission from the large coal-fired power plants in this area (Fig. 1a). Impact of long-range transport from

## Long-term monitoring of atmospheric total gaseous mercury

X. W. Fu et al.

[Title Page](#)

[Abstract](#)

[Introduction](#)

[Conclusions](#)

[References](#)

[Tables](#)

[Figures](#)

◀

▶

◀  
Back

▶  
Close

[Full Screen / Esc](#)

[Printer-friendly Version](#)

[Interactive Discussion](#)



strong source regions of North China tended to decrease in summer, partially because the study area was controlled by the southeast monsoon which brought air masses from ocean areas. On the other hand, the dominant southeast monsoon also carried anthropogenic Hg emission from Korean Peninsula which might be an important source region to the CBS during summer season (Fig. 10b).

## 4 Conclusions

In this study, we conducted multi-year (October 2008–October 2010) continuous measurements of atmospheric TGM at a remote site in Mt. Changbai area, north-eastern China. The mean concentration during the whole sampling campaign was  $1.60 \pm 0.51 \text{ ng m}^{-3}$ . This value is comparable to the values observed from remote areas in the Northern Hemisphere and might be representative of the large-scale mercury background level in northeastern China. This result is much lower than the mean concentration ( $3.58 \pm 1.78 \text{ ng m}^{-3}$ ) observed at the other site in the study area during August 2005 and July 2006. We found that the regional surface wind system changed significantly in these years, with east as the predominant wind direction in this study (October 2008–October 2010) and southwest in the previous study (August 2005–July 2006), respectively. The highly elevated TGM concentrations for the previous study probably resulted from more pronounced impacts of regional sources which were mostly situated to the southwest of the study area. Besides, the sampling site in the previous study was also impacted by coal and biomass Hg emissions from the station and a major settlement nearby.

Both regional sources and long-range transport impacted the distribution of TGM in ambient air at CBS; whereas the effect from local sources was minimal. Regional sources included two large power plants and urban areas situated more than 150 km to the southwest and an iron mining area situated 100 km to the east of the sampling site. The regional sources controlled the diurnal distributions of TGM which showed elevated levels during daytime, and also contributed significantly to the monthly variations

[Title Page](#)[Abstract](#)[Introduction](#)[Conclusions](#)[References](#)[Tables](#)[Figures](#)[◀](#)[▶](#)[◀](#)[▶](#)[Back](#)[Close](#)[Full Screen / Esc](#)[Printer-friendly Version](#)[Interactive Discussion](#)

of TGM. Long-range transported Hg originated mostly from Beijing, Tianjin, northwestern Shanxi, northwestern Shandong, Hebei and southern Liaoning, which were generally regarded as important source regions in China.

- Acknowledgements.* This research was financially supported by INCAPTA project under IPY,  
5 National Science Foundation of China (41003051, 40973086) and Chinese Academy of Science (KZCX2-EW-QN-111). The authors would like to acknowledge Environment Canada for offering the sampling instruments. We thank the Open Research Station of Changbai Mountain Forest Ecosystem, CAS for provide the monitoring platform and meteorological parameters  
10 and Hao Xu, together with other engineers, in the open station who contribute to the mercury measurements.

## References

- Brunke, E.-G., Labuschagne, C., Ebinghaus, R., Kock, H. H., and Slemr, F.: Gaseous elemental mercury depletion events observed at Cape Point during 2007–2008, *Atmos. Chem. Phys.*, 10, 1121–1131, doi:10.5194/acp-10-1121-2010, 2010.  
15 Choi, H. D., Holsen T. M., and Hopke, P. K.: Atmospheric mercury (Hg) in the Adirondacks: Concentrations and sources, *Environ. Sci. Technol.*, 42, 5644–5653, 2008.  
Ci, Z. J., Zhang, X. S., Wang, Z. W., Niu, Z. C., Diao, X. Y., and Wang, S. W.: Distribution and air-sea exchange of mercury (Hg) in the Yellow Sea, *Atmos. Chem. Phys.*, 11, 2881–2892, doi:10.5194/acp-11-2881-2011, 2011.  
20 Engle, M. A., Tate, M. T., Krabbenhoft, D. P., Schauer, J. J., Kolker, A., Shanley, J. B., and Bothner, M. H.: Comparison of atmospheric mercury speciation and deposition at nine sites across central and eastern North America, *J. Geophys. Res.*, 115, D18306, doi:10.1029/2010JD014064, 2010.  
Faïn, X., Obrist, D., Hallar, A. G., Mccubbin, I., and Rahn, T.: High levels of reactive gaseous mercury observed at a high elevation research laboratory in the Rocky Mountains, *Atmos. Chem. Phys.*, 9, 8049–8060, doi:10.5194/acp-9-8049-2009, 2009.  
25 Feng, X., Shang, L., Wang, S., Tang, S., and Zheng, W.: Temporal variation of total gaseous mercury in the air of Guiyang, China, *J. Geophys. Res.*, 109, D03303, doi:10.1029/2003JD004159, 2004.

[Title Page](#)[Abstract](#)[Introduction](#)[Conclusions](#)[References](#)[Tables](#)[Figures](#)[◀](#)[▶](#)[Back](#)[Close](#)[Full Screen / Esc](#)[Printer-friendly Version](#)[Interactive Discussion](#)

## Long-term monitoring of atmospheric total gaseous mercury

X. W. Fu et al.

[Title Page](#)

[Abstract](#)

[Introduction](#)

[Conclusions](#)

[References](#)

[Tables](#)

[Figures](#)



[Back](#)

[Close](#)

[Full Screen / Esc](#)

[Printer-friendly Version](#)

[Interactive Discussion](#)



Fu, X. W., Feng, X. B., Zhu, W. Z., Wang, S. F., and Lu, J.: Total gaseous mercury concentrations in ambient air in the eastern slope of Mt. Gongga, South-Eastern fringe of the Tibetan plateau, China, *Atmos. Environ.*, 42, 70–979, 2008.

Fu, X. W., Feng, X. B., Wang, S. F., Rothenberg, S., Shang, L. H., Li, Z. G., and Qiu, G. L.: Temporal and spatial distributions of total gaseous mercury concentrations in ambient air in a mountainous area in southwestern China: Implications for industrial and domestic mercury emissions in remote areas in China, *Sci. Total. Environ.*, 407, 2306–2314, 2009.

Fu, X. W., Feng, X., Dong, Z. Q., Yin, R. S., Wang, J. X., Yang, Z. R., and Zhang, H.: Atmospheric gaseous elemental mercury (GEM) concentrations and mercury depositions at a high-altitude mountain peak in south China, *Atmos. Chem. Phys.*, 10, 2425–2437, doi:10.5194/acp-10-2425-2010, 2010.

Fu, X. W., Feng, X., Liang, P., Deli-Geer, Zhang, H., Ji, J., and Liu, P.: Temporal trend and sources of speciated atmospheric mercury at Waliguan GAW station, northwestern China, *Atmos. Chem. Phys. Discuss.*, 11, 30053–30089, doi:10.5194/acpd-11-30053-2011, 2011.

Kellerhals, M., Beauchamp, S., Belzer, W., Blanchard, P., Froude, F., Harvey, B., McDonald, K., Pilote, M., Poissant, L., Puckett, K., Schroeder, B., Steffen, A., and Tordon, R.: Temporal and spatial variability of total gaseous mercury in Canada: results from the Canadian Atmospheric Mercury Measurement Network (CAMNet), *Atmos. Environ.*, 37, 1003–1011, 2003.

Kim, E., Hopke, P. K., Henski, M., and Koerber, M.: Source of fine particles in a rural Midwestern U.S., area, *Environ. Sci. Technol.*, 39, 4953–4960, 2005.

Kock, H. H., Bieber, E., Ebinghaus, R., Spain, T. G., and Thees, B.: Comparison of long-term trends and seasonal variations of atmospheric mercury concentrations at the two European coastal monitoring stations Mace Head, Ireland and Zingst, Germany, *Atmos. Environ.*, 39, 7549–7556, 2005.

Lee, D. S., Dollard, G. J., and Pepler, S.: Gas-phase mercury in the atmosphere of the United Kingdom, *Atmos. Environ.*, 32, 855–864, 1998.

Li, G. H., Feng, X. B., Li, Z. G., Qiu, G. L., Shang, L. H., Liang, P., Wang, D. Y., and Yang, Y. K.: Mercury emission to atmosphere from primary Zn production in China, *Sci. Total Environ.*, 408, 4607–4612, 2010.

Li, P., Lin, C. J., Carmichael, G. R., Street, D. G., Tang, Y. H., Woo, J. H., Shetty, S. K., Chu, H. W., Ho, T. C., Friedli, H. R., and Feng, X. B.: Study of atmospheric Hg budget in East Asia using STEM-Hg modeling system, *Sci. Total. Environ.*, 408, 3277–3291, 2010.

- Lin, C.-J., Pan, L., Streets, D. G., Shetty, S. K., Jang, C., Feng, X., Chu, H.-W., and Ho, T. C.: Estimating mercury emission outflow from East Asia using CMAQ-Hg, *Atmos. Chem. Phys.*, 10, 1853–1864, doi:10.5194/acp-10-1853-2010, 2010.

Lindberg, S., Bullock, R., Ebinghaus, R., Engstrom, D., Feng, X., Fitzgerald, W., Pirrone, N., Prestbo, E., and Seigneur, Ch.: A synthesis of progress and uncertainties in attributing the sources of mercury in deposition, *Ambio*, 36, 19–32, 2007.

Liu, S., Nadim, F., Perkins, C., Carley, R. J., Hoag, G. E., Lin, Y. H., and Chen, L. T.: Atmospheric mercury monitoring survey in Beijing, China, *Chemos.*, 48, 97–107, 2002.

Mao, H., Talbot, R. W., Sigler, J. M., Sive, B. C., and Hegarty, J. D.: Seasonal and diurnal variations of  $Hg^0$  over New England, *Atmos. Chem. Phys.*, 8, 1403–1421, doi:10.5194/acp-8-1403-2008, 2008.

Nguyen, H. T., Kim, K. H., Kim, M. Y., Hong, S., Youn, Y. H., Shon Z. H., and Lee, J. S.: Monitoring of atmospheric mercury at a Global Atmospheric Watch (GAW) site on An-Myun Island, Korea, *Water Air Soil Pollut.*, 185, 149–164, 2007.

Pacyna, E. G., Pacyna, J. M., Sundseth, K., Munthe, J., Kindbom, K., Wilson, S., Steenhuisen, F., and Maxon, P.: Global emission of mercury to the atmosphere from anthropogenic sources in 2005 and projections of 2020, *Atmos. Environ.*, 44, 2484–2499, 2010.

Pirrone, N., Cinnirella, S., Feng, X., Finkelman, R. B., Friedli, H. R., Leaner, J., Mason, R., Mukherjee, A. B., Stracher, G. B., Streets, D. G., and Telmer, K.: Global mercury emissions to the atmosphere from anthropogenic and natural sources, *Atmos. Chem. Phys.*, 10, 5951–5964, doi:10.5194/acp-10-5951-2010, 2010.

Poissant, L., Pilote, M., Beauvais, C., Constant, P., and Zhang, H. H.: A year of continuous measurements of three atmospheric mercury species (GEM,RGM and HgP) in southern Québec, Canada, *Atmos. Environ.*, 39, 1275–1287, 2005.

Poissant, L., Pilote, M., Yumvihoze, E., and Lean, D.: Mercury concentrations and foliage-atmosphere fluxes in a maple forest ecosystem in Québec, Canada, *J. Geophys. Res.*, 113, D10307, doi:10.1029/2007JD009510, 2008.

Polissar, A. V., Hopke, P. K., and Harris, J. M.: Source regions for atmospheric aerosol measured at Barrow, Alaska, *Environ. Sci. Technol.*, 35, 4214–4226, 2001.

Schroeder, W. H. and Munthe, J.: Atmospheric mercury - an overview, *Atmos. Environ.*, 5, 809–822, 1998.

Shetty, S. K., Lin, C. J., Streets, D. G., and Jang, C.: Model estimate of mercury emission from natural sources in East Asia, *Atmos. Environ.*, 42, 8674–8685, 2008.

# Long-term monitoring of atmospheric total gaseous mercury

X. W. Fu et al.

Title Page

## Abstract

Introduction

## Conclusions

## References

Tables

## Figures

1

▶

Bac

**Close**

Full Screen / Esc

[Printer-friendly Version](#)

## Interactive Discussion



Slemer, F., Brunke, E. G., Labuschagne, C., and Ebinghaus, R.: Total gaseous mercury concentrations at the the Cape Point GAW station and their seasonality, *Geophys. Res. Lett.*, 35, L11807, doi:10.1029/2008GL033741, 2008.

Slemer, F., Ebinghaus, R., Brenninkmeijer, C. A. M., Hermann, M., Kock, H. H., Martinsson, B. G., Schuck, T., Sprung, D., van Velthoven, P., Zahn, A., and Ziereis, H.: Gaseous mercury distribution in the upper troposphere and lower stratosphere observed onboard the CARIBIC passenger aircraft, *Atmos. Chem. Phys.*, 9, 1957–1969, doi:10.5194/acp-9-1957-2009, 2009.

Swartzendruber, P. C., Jaffe, D. A., Prestbo, E. M., Weiss-Penzias, P., Selin, N. E., Park, R., Jacob, D. J., Strode, S., and Jaegle, L.: Observations of reactive gaseous mercury in the free troposphere at the Mount Bachelor Observatory, *J. Geophys. Res.*, 111, D24302, doi:10.1029/2006jd007415, 2006.

Temme, C., Slemer, F., Ebinghaus, R., and Einax, J. W.: Distribution of mercury over the Atlantic Ocean in 1996 and 1999–2001, *Atmos. Environ.*, 37, 1889–1897, 2003.

Valente, R. J., Shea, C., Lynn Humes, K., and Tanner, R. L.: Atmospheric mercury in the Great Smoky Mountains compared to regional and global levels, *Atmos. Environ.*, 41, 1861–1873, 2007.

Wan, Q., Feng, X. B., Julia, L., Zheng, W., Song, X. J., Han, S. J., and Xu, H.: Atmospheric mercury in Changbai Mountain area, northeastern China - Part 1: The seasonal distribution pattern of total gaseous mercury and its potential sources, *Environ. Res.*, 109, 201–206, 2009.

Wang, S. F., Jia, Y. F., Wang, S. Y., Wang, X., Wang, H., Zhao, Z. X., and Liu, B. Z.: Total mercury and monomethylmercury in water, sediments, and hydrophytes from the reveres, estuary, and bay along the Bohai Sea coast, northeastern China, *Appl. Geochem.*, 24, 1702–1711, 2009.

Wang, Y. Q., Zhang, X. Y., and Draxler, R. R.: TrajStat: GIS-based software that uses various trajectory statistical analysis methods to identify potential sources from long-term air pollution measurement data, *Environ. Model. Soft.*, 24, 938–939, 2009.

Wilson, S. J., Steenhuisen, F., Pacyna, J. M., and Pacyna, E. G.: Mapping the spatial distribution of global anthropogenic mercury atmospheric emission inventories, *Atmos. Environ.*, 40, 4621–4632, 2006.

Wu, Y., Wang, S. X., Streets, D. G., Hao, F. M., Chan, M., and Jiang, J. K.: Trends in Anthropogenic Mercury Emissions in China from 1995 to 2003, *Environ. Sci. Technol.*, 40,

## Long-term monitoring of atmospheric total gaseous mercury

X. W. Fu et al.

[Title Page](#)

[Abstract](#)

[Introduction](#)

[Conclusions](#)

[References](#)

[Tables](#)

[Figures](#)



[Back](#)

[Close](#)

[Full Screen / Esc](#)

[Printer-friendly Version](#)

[Interactive Discussion](#)



5312–5318, 2007.

Zhang, H.: Concentrations of speciated atmospheric mercury at a high-altitude background station in the Shangri-La area of Tibetan Plateau, China, Abstract to 10th international conference on Mercury as a global pollutant, Halifax, Canada, 2011.

ACPD

12, 4417–4446, 2012

---

Long-term  
monitoring of  
atmospheric total  
gaseous mercury

X. W. Fu et al.

---

<a href="#">Title Page</a>	
<a href="#">Abstract</a>	<a href="#">Introduction</a>
<a href="#">Conclusions</a>	<a href="#">References</a>
<a href="#">Tables</a>	<a href="#">Figures</a>
<a href="#">◀</a>	<a href="#">▶</a>
<a href="#">◀</a>	<a href="#">▶</a>
<a href="#">Back</a>	<a href="#">Close</a>
<a href="#">Full Screen / Esc</a>	
<a href="#">Printer-friendly Version</a>	
<a href="#">Interactive Discussion</a>	

Discussion Paper | Discussion Paper

Discussion Paper | Discussion Paper

Discussion Paper | Discussion Paper

**Table 1.** Summary of TGM concentrations ( $\text{ng m}^{-3}$ ) at CBS.

	Mean	Median	Std	10th	90th	Range	N
Spring	1.61	1.51	0.45	1.16	2.20	0.37–8.13	43 371
Summer	1.52	1.45	0.56	0.90	2.33	<DI–5.31	37 821
Autumn	1.64	1.45	0.64	1.04	2.42	<DI–9.50	37 363
Winter	1.61	1.48	0.47	1.16	2.24	0.51–6.60	45 615
Total	1.60	1.48	0.51	1.08	2.29	<DI–9.50	164 170



# Long-term monitoring of atmospheric total gaseous mercury

X. W. Fu et al.

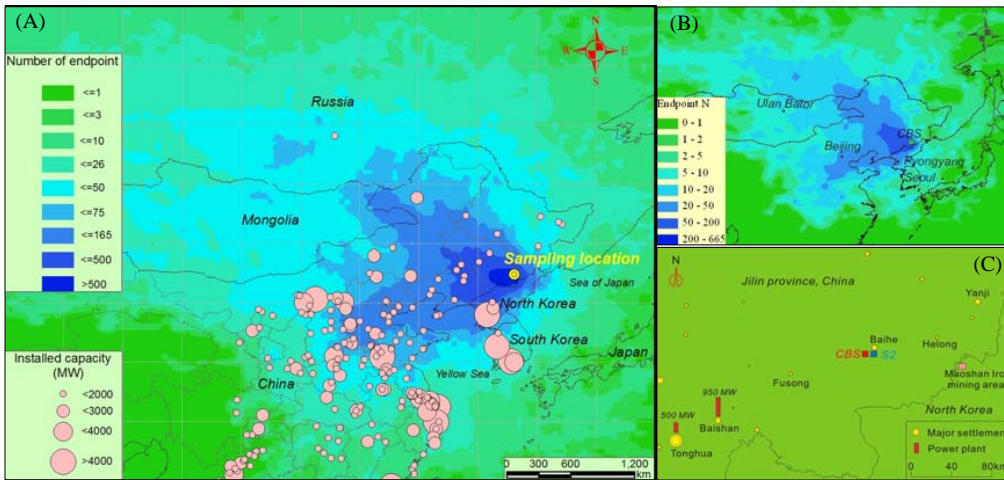


**Fig. 1.** Map showing **(A)** location of the sampling site, large coal-fired power plants and air masse endpoints at CBS during the year of October 2008–October 2010; **(B)** endpoints at the site of S2 during August 2005 and July 2006; and **(C)** regional major settlements and large point sources in Mt. Changbai area.

Title Page

## Abstract

Introduction

## Conclusions

## References

Tables

## Figures

## Tables | Figures

## Figures

Tables | Figures

## Figures

1

1

▶

Back

**Close**

Full Screen / Esc

[Printer-friendly version](#)

## Interactive Discussion

**Long-term  
monitoring of  
atmospheric total  
gaseous mercury**

X. W. Fu et al.

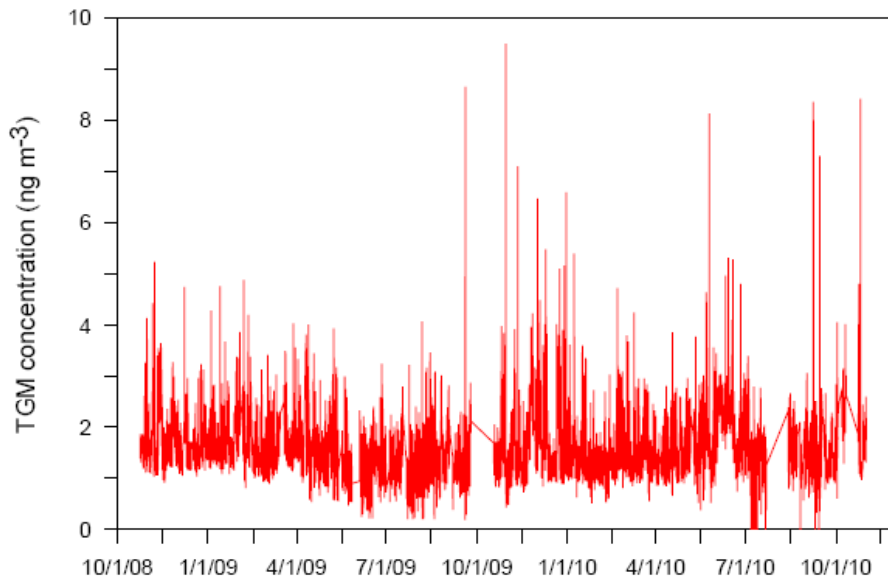


**Fig. 2.** Time series of TGM concentrations at CBS.

- [Title Page](#)
- [Abstract](#) [Introduction](#)
- [Conclusions](#) [References](#)
- [Tables](#) [Figures](#)
- [◀](#) [▶](#)
- [◀](#) [▶](#)
- [Back](#) [Close](#)
- [Full Screen / Esc](#)
- [Printer-friendly Version](#)
- [Interactive Discussion](#)

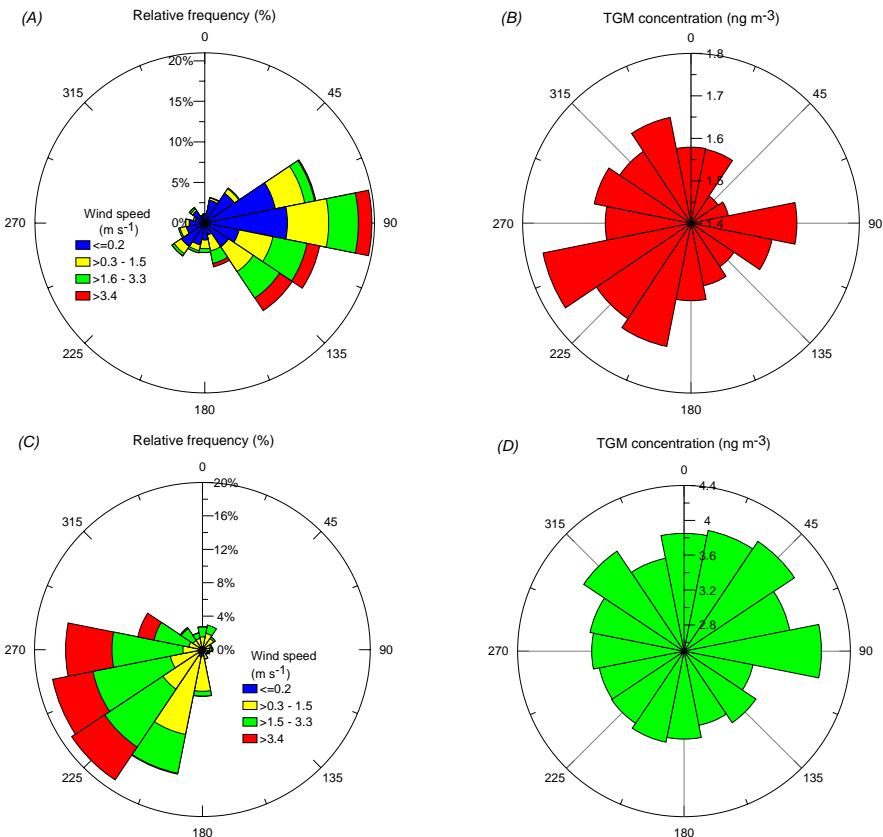


**Fig. 3.** (A) Wind rose at CBS during October 2008 and October 2010; (B) directional dependence of TGM concentrations at CBS during October 2008 and October 2010; (C) wind rose at S2 during August 2005 and July 2006; and (D) directional dependence of TGM at S2 during August 2005 and July 2006.

## Long-term monitoring of atmospheric total gaseous mercury

X. W. Fu et al.

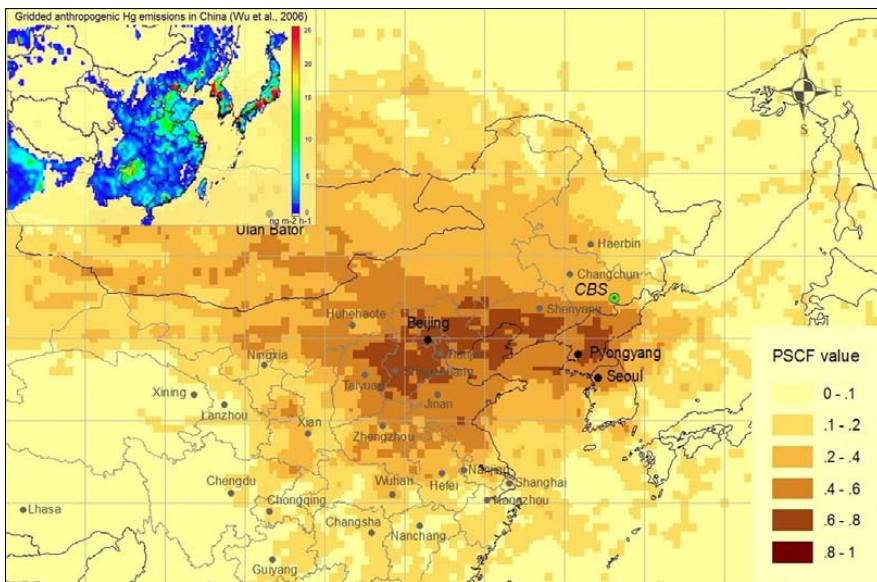


**Fig. 4.** Likely potential source areas identified by PSCF analysis at CBS for the whole study period.

- [Title Page](#)
- [Abstract](#) [Introduction](#)
- [Conclusions](#) [References](#)
- [Tables](#) [Figures](#)
- [◀](#) [▶](#)
- [◀](#) [▶](#)
- [Back](#) [Close](#)
- [Full Screen / Esc](#)
- [Printer-friendly Version](#)
- [Interactive Discussion](#)



# Long-term monitoring of atmospheric total gaseous mercury

X. W. Fu et al.

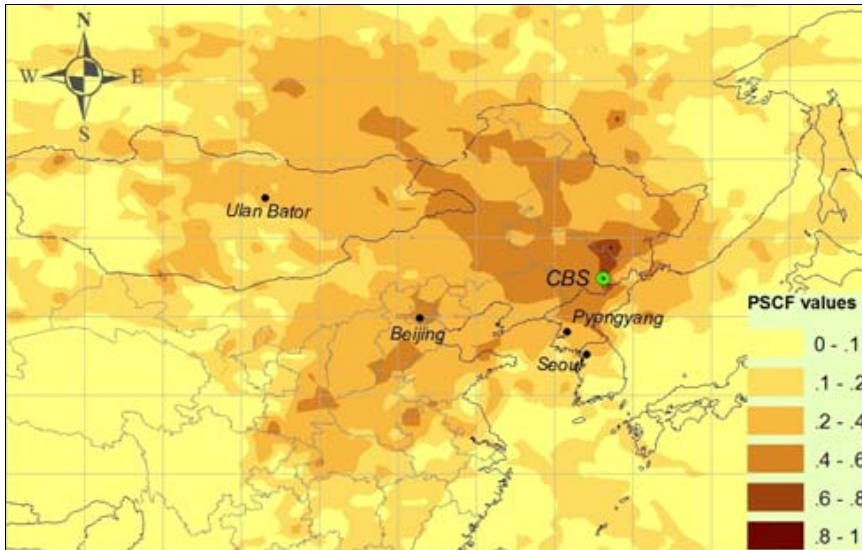


**Fig. 6.** Likely potential areas at S2 during August 2005 and July 2006.

Title Page

## Abstract

Introduction

## Conclusions

## References

## Tables

## Figures

1

▶

1

1

Full Screen / Esc

[Printer-friendly Version](#)

### Interactive Discussion



# Long-term monitoring of atmospheric total gaseous mercury

X. W. Fu et al.

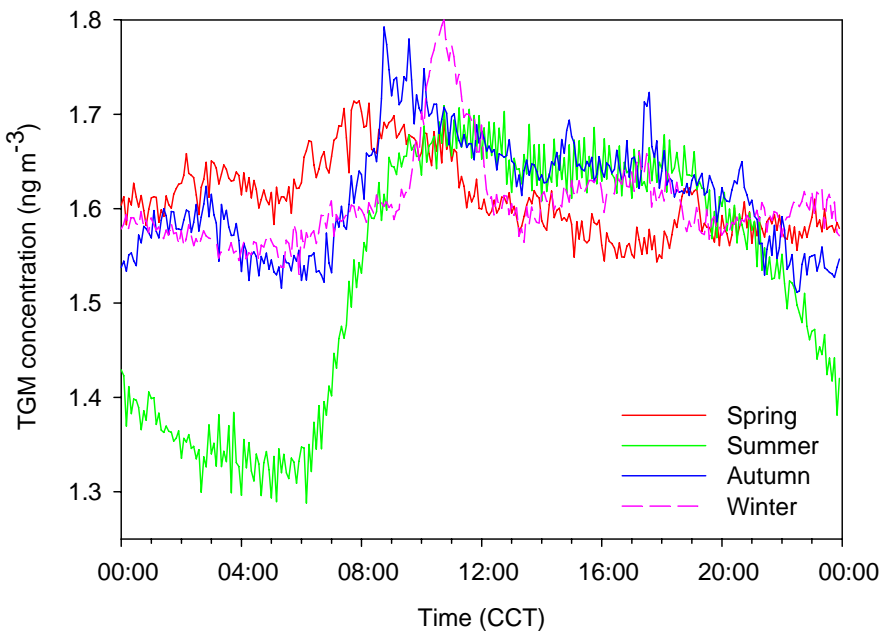


**Fig. 7.** Seasonal diurnal variations of TGM at CBS.

Title Page

Abstra

Introduction

## Conclusi

## References

Tables

Figures



Back

Close

Full Screen / Esc

[Printer-friendly Version](#)

## Interactive Discussion



# Long-term monitoring of atmospheric total gaseous mercury

X. W. Fu et al.

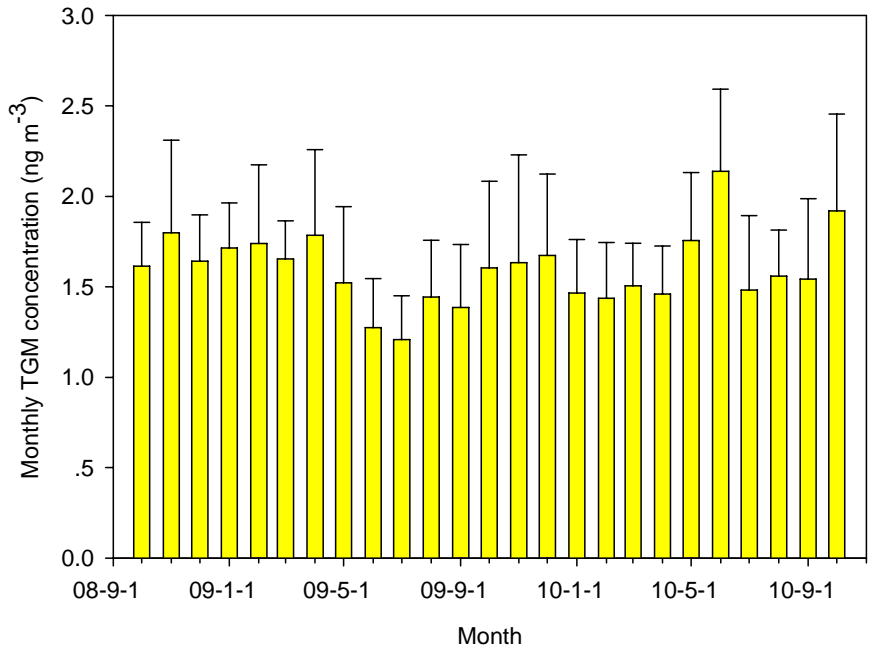


**Fig. 8.** Monthly variations of TGM at CBS.

Title Page

Abstra

Introduction

Conclusi

## References

Tables

## Figures

1

1

◀

1

Back

**Close**

Full Screen / Esc

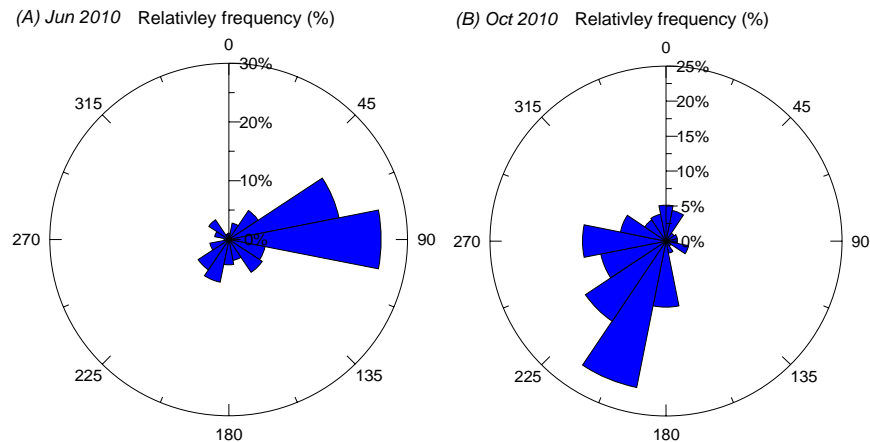
[Printer-friendly Version](#)

## Interactive Discussion



**Long-term  
monitoring of  
atmospheric total  
gaseous mercury**

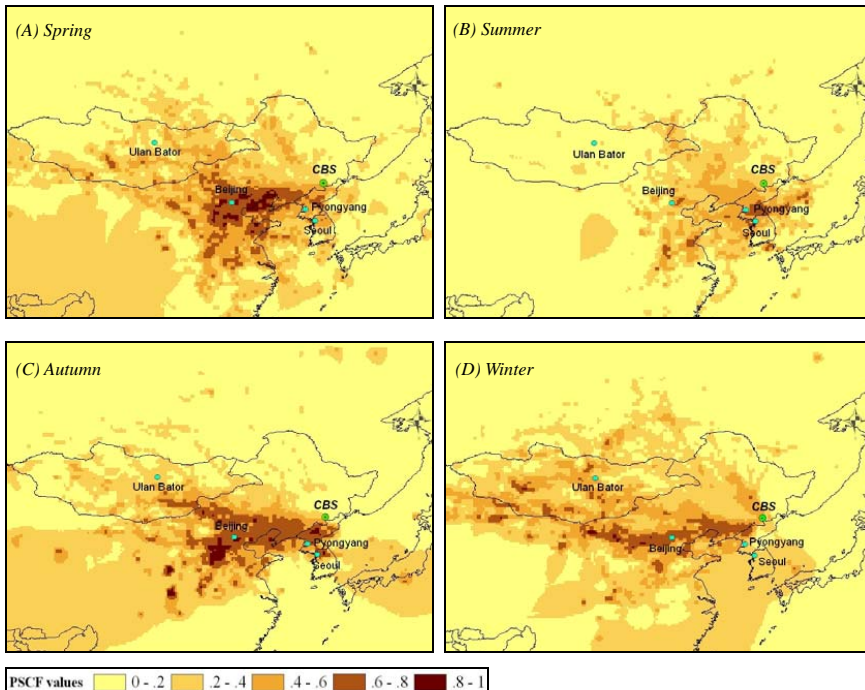
X. W. Fu et al.



**Fig. 9.** Wind rose at CBS in (A) June 2010 and (B) October 2010.

**Long-term  
monitoring of  
atmospheric total  
gaseous mercury**

X. W. Fu et al.

**Fig. 10.** Seasonal PSCF results of TGM at CBS.[Title Page](#)[Abstract](#)[Introduction](#)[Conclusions](#)[References](#)[Tables](#)[Figures](#)[Back](#)[Close](#)[Full Screen / Esc](#)[Printer-friendly Version](#)[Interactive Discussion](#)